Synergistic value of fractional flow reserve and low-density non-calcified plaque based on coronary computed tomography angiography for the identification of lesion-specific ischemia

LIN-MENG TANG[1*], FENG LIU[1*], TING-YU DONG[1], FEI YANG[1,2] and SHU-JUN CUI[1,2]

[1]Graduate School, Hebei North University; [2]Department of Medical Imaging, The First Affiliated Hospital of Hebei North University, Zhangjiakou, Hebei 075000, P.R. China

Received June 16, 2022; Accepted September 14, 2022

DOI: 10.3892/etm.2022.11637

Abstract. Increasing evidence has suggested that plaque characteristics are closely associated with ischemia, and coronary computed tomography (CT) angiography-derived fractional flow reserve (FFR_{CT}) based on deep machine learning algorithms has also been used to identify lesion-specific ischemia. Therefore, the aim of the present study was to explore the predictive ability of plaque characteristics in combination with deep learning-based FFR_{CT} for lesion-specific ischemia. To meet this end, invasive FFR was used as a reference standard, with the joint aims of the early prediction of ischemic lesions and guiding clinical treatment. In the present study, the plaque characteristics, including non-calcified plaque (NCP), low-density NCP (LD-NCP), plaque length, total plaque volume (TPV), remodeling index, calcified plaque, fibrous plaque and plaque burden, were obtained using a semi-automated program. The FFR_{CT} values were derived based on a deep machine learning algorithm. On the basis of the data obtained, differences among the values between the atopic ischemia and the non-significant lesions groups were analyzed to further determine the predictive value of independent predictors for atopic ischemia. Of the plaque features, FFR_{CT}, LD-NCP, NCP, TPV and plaque length differed significantly when comparing between the lesion-specific ischemia and no hemodynamic abnormality groups, and LD-NCP and FFR_{CT} were both independent predictors for ischemia. Additionally, FFR_{CT} combined with LD-NCP showed a greater ability at discriminating ischemia compared with FFR_{CT} or LD-NCP alone. Taken together, the findings of the present study suggest that the combination of FFR_{CT} and LD-NCP has a synergistic effect in terms of predicting ischemia, thereby facilitating the identification of specific ischemia in patients with coronary artery disease.

Correspondence to: Professor Shu-Jun Cui, Department of Medical Imaging, The First Affiliated Hospital of Hebei North University, 12 Changqing Road, Qiaoxi, Zhangjiakou, Hebei 075000, P.R. China
E-mail: hbzjkcsj@163.com

*Contributed equally

Key words: fractional flow reserve, ischemia, low-density non-calcified plaque, plaque characteristics, computed tomography angiography

Introduction

A non-reversible imbalance in myocardial blood supply and demand results in myocardial ischemia in patients with coronary artery disease (CAD), which can further lead to heart failure and myocardial infarction. CAD is currently a major cause of death worldwide, with 31% of all deaths resulting from it (1). During invasive coronary radiography, fractional flow reserve (FFR) is measured, and this is used as a gold standard for determining myocardial ischemia caused by coronary stenosis. However, both its invasive nature and the risk of complications serve to limit its clinical applicability (2). Coronary computed tomography (CT) angiography (CCTA) is recognized as the most accurate means for excluding CAD (3). Nevertheless, a purely anatomical assessment of hemodynamics is hardly able to provide sufficient guidance for clinical treatment.

Currently, the application of non-invasive techniques to assess myocardial ischemia due to abnormal coronary hemodynamics reduces the occurrence of adverse cardiac events. FFR obtained by CCTA (FFR_{CT}), based on deep machine learning algorithms, has been shown to be an effective assessment method for detecting ischemia, demonstrating a high diagnostic performance compared with invasive FFR (4-6). Additionally, when CCTA-derived plaque characteristics and composition have been obtained using a semi-automated program, this has been shown to improve the ability of CCTA to predict hemodynamic abnormalities by obtaining more information about the lesion (7,8). Previous studies have also suggested that low-density non-calcified plaque (LD-NCP) acts as a substitute for the necrotic lipid core, and the larger its volume, the higher the possibility of ischemia (9,10). However, the potential of quantitative CCTA-derived plaque combined with FFR_{CT} for lesion-specific ischemia detection needs to be explored further. To meet this end, the present study aimed

to evaluate the predictive performance of deep learning-based FFR_{CT} in combination with CCTA-derived plaque characteristics for identifying lesion-specific ischemia according to the gold standard of invasive FFR.

Materials and methods

Study population. The present study was a retrospective study conducted at a single center. A total of 144 patients with coronary heart disease admitted to The First Affiliated Hospital of Hebei North University (Zhangjiakou, China) between February 2019 and March 2022 were included in the current study. Invasive coronary angiography (ICA) and CCTA were both performed on all patients, and the interval between the two examinations was ≤30 days. The inclusion criteria were as follows: i) Complete clinical data and CCTA images were available for the patient; and ii) these were of sufficient quality for FFR_{CT} and plaque analysis. The exclusion criteria were as follows: i) Poor coronary CTA image quality; ii) patients who had previously undergone revascularization procedures (for example, cardiac bypass graft and/or percutaneous coronary intervention); iii) the patient had contraindications to adenosine, nitrates or β-blockers; and iv) the patient had been diagnosed with a combination of severe cardiovascular disease (for example, severe arrhythmias and/or severe heart failure). The current study was approved by the Ethics Committee of The First Affiliated Hospital of Hebei North University (Zhangjiakou, China; approval no. K2020237), and written informed consent was obtained from all of the participants.

ICA and FFR techniques. ICA and FFR were performed in accordance with standard practices (11). The FFR pressure-wire was placed at least 20 mm distal to the ≥2 mm vessel stenosis after ICA. Adenosine (140-180 μg/kg/min; Pfizer, Inc.) was used to induce hyperemia, and both the distal coronary pressure (Pd) and the aortic pressure (Pa) were measured simultaneously at baseline and during maximal hyperemia. Based on a beat-to-beat calculation, the FFR was determined as the mean Pd divided by the mean Pa at maximal hyperemia. Lesion-specific ischemia was defined upon calculating a FFR value of ≤0.80.

CCTA acquisition. CCTA was performed using an Aquilion ONE ViSION CT scanner (320-MDCT; Canon Medical Systems Corporation). Nitroglycerin (0.8 mg; Xinyi Pharmaceutical Co., Ltd.) was given sublingually to all patients prior to the CT scan, and patients whose heart rate pre-scan was >60 beats/min were administered metoprolol (AstraZeneca Pharmaceutical Co., Ltd.) orally (20-40 mg), with the heart rate held at ≤60 beats/min. The isotonic contrast agent, iodixanol (320 mg iodine/ml; Jiangsu Hengrui Medicine Co., Ltd.), was injected at a rate of 5.5 ml/sec using a double-barrel hyperbaric syringe, followed immediately by injection of 30 ml of 0.9% sodium chloride solution at the same rate. Regarding the scan parameters, the tube voltage was set at 100 kV, and the tube current was automatically modulated. Monitoring was set in the descending aorta at the level of 1 cm below the tracheal bifurcation. The scan was automatically triggered using SUREStart™ software (version 1.0; Canon Medical Systems Corporation) when 200 Hounsfield units (HU) were reached, ranging from below the tracheal ridge to the diaphragm surface, and the clearest coronary image was selected for reconstruction. The CCTA images were analyzed and processed by two physicians with professional diagnostic imaging qualifications in the Department of Medical Imaging, The First Affiliated Hospital of Hebei North University. The two physicians were blinded to the clinical information and CCTA results of the patients, and differences in the assessment results were re-evaluated by a third experienced physician, before subsequently being discussed to obtain the final results. The branches of the stenotic coronary arteries [i.e., the left anterior descending artery (LAD), the left circumflex artery (LCX) and the right coronary artery (RCA)] were observed.

Coronary plaque analysis. The scan-specific algorithm, Vitrea FX version 4.0 (Vital Images; Canon Medical Systems Corporation), was used to assess the plaque characteristics for each coronary lesion segment ≥2 mm. By using this automated method, CCTA was able to rapidly measure plaque features (12). Vitrea FX utilizes multiplanar CCTA images to identify the proximal and distal center points of each lesion, and then the vessel borders and plaque are automatedly segmented. For each lesion, plaque volumes were measured for the following subtypes of plaque: Total plaque, fibrous plaque, calcified plaque (CP), NCP and LD-NCP (the latter was defined as attenuation <30 HU). NCP was further classified by plaque HU into two components: Necrotic core (-30 to 30 HU) and fibrous plaque (131 to 350 HU) (13,14). Semi-quantitative measurements were conducted at the region of maximal stenosis degree to determine the diameter of the minimal lumen. To calculate the remodeling index (RI), the cross-sectional vessel area at the site of greatest stenosis was divided by the mean cross-sectional vessel area at the proximal point of the reference. The plaque burden was calculated according to the plaque volume divided by the vessel volume of the analyzed coronary lesion (i.e., plaque volume/vessel volume x100). The presence of the napkin-ring sign, defined as a low-density plaque core surrounded by high-density areas (15), was investigated. Spotty calcifications were defined as calcified plaque of length <3 mm within a lesion (16). The volumes and characteristics of coronary plaques were assessed for each patient and for each vessel.

Deep learning-based FFR_{CT}. FFR_{CT} measurements were conducted using deep learning-based DEEPVESSEL® FFR software (version 1.0; Beijing Keya Medical Technology Co., Ltd.), and the CCTA images of the patients were uploaded to its image-computing platform using Digital Imaging and Communications in Medicine (DICOM), the standard for the communication and management of medical imaging information and associated data. The system automatically calculated the FFR_{CT} value of each coronary artery via a hydrodynamic model (17), which was presented as a color coronary tree, with different colors indicating different FFR_{CT} values. FFR_{CT} values ≤0.80 were considered to be indicative of lesion-specific ischemia (18).

Statistical analysis. The continuous variables are expressed as the mean ± standard deviation (SD) or median (interquartile range), whereas categorical variables are expressed as numbers (percentages). As required, unpaired Student's t-test, Pearson's

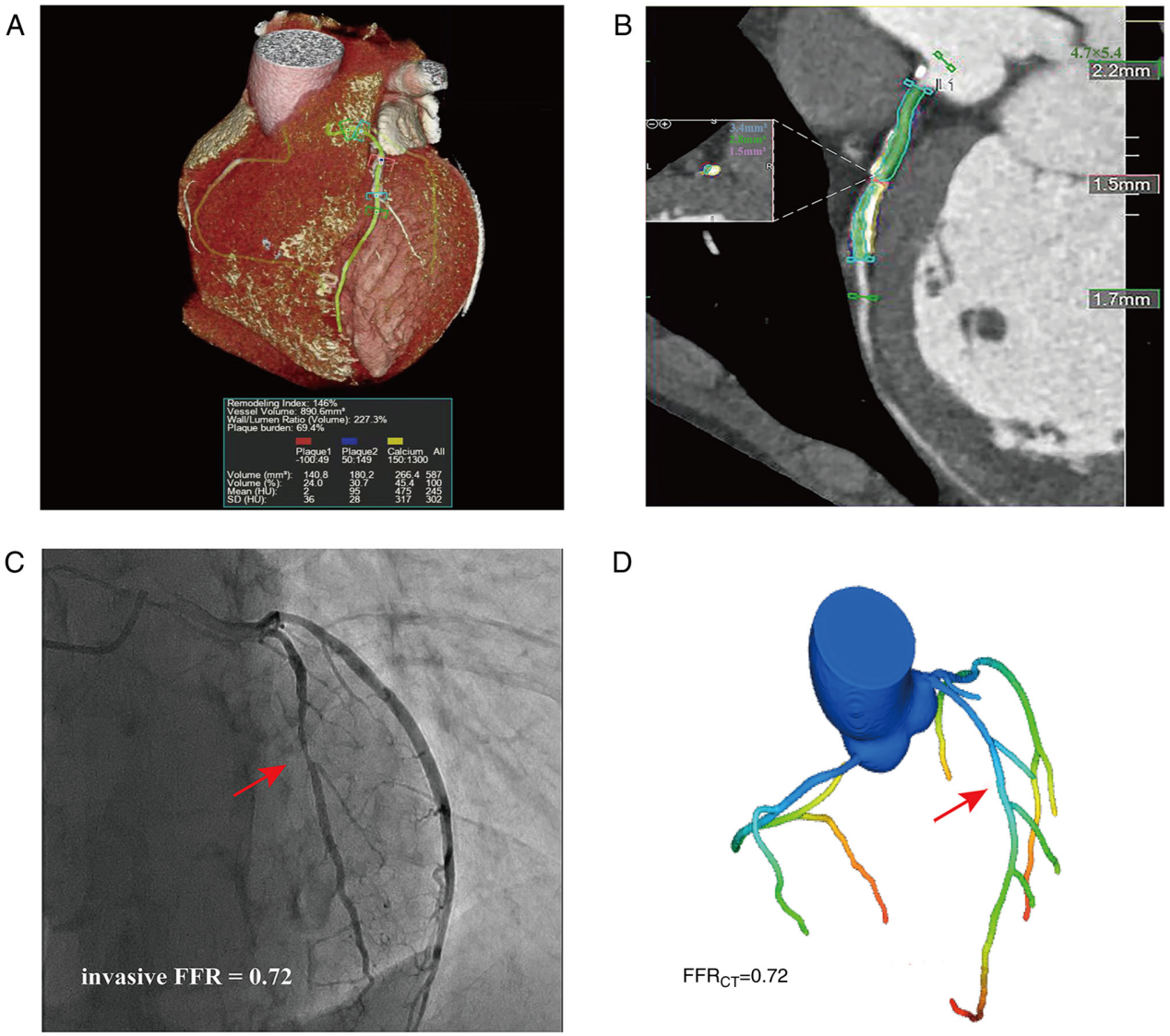

Figure 1. Case example of a 61-year-old male. (A) Coronary computed tomography angiography demonstrating a stenotic plaque of the LAD in a 3D imaging scan, revealing the mixed plaque composition of the proximal portion of the LAD: Calcified plaque, 266.4 mm^3 (yellow); non-calcified plaque, 180.2 mm^3 (blue); and low-density non-calcified plaque, 140.8 mm^3 (red). (B) Color-coded semi-automatic plaque quantification of the lesion, as determined by (C) invasive coronary angiography, showing 50% stenosis of the LAD (red arrow), with the measured invasive FFR being 0.72. (D) Three-dimensional color-coding, revealing that FFR$_{CT}$ in the distal LAD was 0.72. LAD, left anterior descending artery; FFR, fractional flow reserve; FFR$_{CT}$, computed tomography angiography-derived FFR; SD, standard deviation; HU, Hounsfield units.

χ^2 test or Mann-Whitney U-test were used for data comparisons. To determine the predictors of ischemia, logistic regression analysis was conducted (for FFR$_{CT}$ values ≤0.80). Receiver operating characteristic (ROC) curves and the area under the curve (AUC) were used to evaluate the predictive values of FFR$_{CT}$, LD-NCP, and the combination of FFR$_{CT}$ and LD-NCP for lesion-specific ischemia, and pairwise comparisons of AUC were made using the DeLong test (19). P<0.05 with a 95% confidence interval (CI) was considered to indicate a statistically significant difference. All of the statistical analyses were conducted using SPSS software, version 26.0 (IBM Corp.) and MedCalc software, version 20 (MedCalc Software bvba).

Results

Patient characteristics. In the study population, 144 patients with 243 vessels were investigated by FFR (Fig. 1). The mean age (± SD) of the patients was 62.0±5.4 years, the mean body mass index (± SD) was 25.0±1.5 kg/m^2 and 96/144 (66.7%) of the participants were male. Regarding risk factors for coronary heart disease, 67/144 (46.5%) of the patients had hypertension, 43/144 (29.9%) had diabetes, 76/144 (52.8%) had hyperlipidemia and 47/144 (32.6%) had a history of smoking. All patients underwent ICA within 30 days of CCTA, with a mean interval (± SD) of 19.1±5.8 days. Of the 243 vessels, 136/243 (56.0%) were the LAD, 57/243 (23.5%) were the RCA and 50/243 (20.6%) were the LCX. The basic characteristics of the included study population are shown in Table I.

Association of plaque characteristics and lesion-specific ischemia. Associations between plaque characteristics and lesion-specific ischemia were evaluated. The plaque characteristics RI, CP, fibrous plaque volume, plaque burden, napkin-ring sign, spotty calcifications and stenosis >50%

Table I. Basic characteristics of all study patients.

Characteristic	FFR ≤0.80 (n=82)	FFR >0.8 (n=62)	P-value	Total (n=144)
Age, years[a]	61±5.8	63±4.7	0.065[b]	62±5.4
Male sex, n (%)	60 (73.2)	36 (58.1)	0.057[c]	96 (66.7)
Body mass index, kg/m^2[a]	24±2.8	25±1.4	0.877[b]	25±1.5
Presence of hypertension, n (%)	37 (45.1)	30 (48.4)	0.679[c]	67 (46.5)
Presence of diabetes mellitus, n (%)	24 (29.3)	19 (30.6)	0.858[c]	43 (29.9)
Presence of dyslipidemia, n (%)	46 (56.1)	30 (48.4)	0.359[c]	76 (52.8)
History of smoking, n (%)	24 (29.3)	20 (32.3)	0.700[c]	47 (32.6)
Period from CCTA to invasive coronary angiography, days[a]	19.5±5.7	18.7±5.9	0.447[b]	19.1±5.8
Vascular level[d]				
Left anterior descending artery, n (%)	79 (55.2)	67 (67.0)	0.066[c]	136 (56.0)
Left circumflex artery, n (%)	25 (17.5)	25 (25.0)	0.154[c]	50 (20.6)
Right coronary artery, n (%)	39 (27.3)	18 (18.0)	0.093[c]	57 (23.5)

[a]Mean ± SD. [b]Comparisons made using Student's t-test. [c]Comparisons made using Pearson's χ^2 test. The displayed P-values refer to comparisons between the basic characteristics of the FFR <0.80 group and the FFR >0.80 group. [d]n=143 for the FFR <0.80 group and n=100 for the FFR >0.80 group. FFR, fractional flow reserve; CCTA, coronary computed tomography angiography.

Table II. Plaque characteristics and FFR_{CT} according to lesion-specific ischemia (FFR ≤0.80).

Characteristic	Overall (n=243)	FFR ≤0.80 (n=143)	FFR >0.80 (n=100)	P-value
FFR_{CT}	0.81±0.08	0.76±0.07	0.86±0.04	<0.0001[a]
Remodeling index	1.08 (0.74)	1.1 (0.46)	1.07 (0.74)	0.293[c]
Calcified plaque (mm^3)	72.9±12.6	74.0±11	71.0±14.7	0.074[b]
Non-calcified plaque (mm^3)	255±44	286±23	210±22	<0.0001[a]
Low-density non-calcified plaque (mm^3)	46±14	53±13	35±11	<0.0001[a]
Total plaque volume (mm^3)	268±71	275±82	257±50	0.031[a]
Fibrous plaque volume (mm^3)	58.4±11.5	59.2±11.0	57.0±12.0	0.167[b]
Plaque length (mm)	16.5±2.9	17.0±3.2	15.9±2.3	0.002[a]
Plaque burden, n (%)	104 (66)	104 (65)	101 (67)	0.051[c]
Napkin ring sign, n (%)	58 (23.9)	37 (25.9)	21 (21.0)	0.38[b]
Spotty calcification, n (%)	54 (22.2)	34 (23.8)	20 (20.0)	0.486[b]
Stenosis >50%, n (%)	144 (59.3)	91 (63.6)	53 (53.0)	0.097[b]

[a]P<0.05; [b]compared using Student's t-test; [c]comparisons made using Pearson's χ^2 test. FFR, fractional flow reserve; FFR_{CT}, coronary computed tomography angiography-derived fractional flow reserve.

showed no significant differences when comparing between lesion-specific ischemia and non-significant lesions (P>0.05). By contrast, NCP, LD-NCP, total plaque volume and plaque length were significantly different in lesion-specific ischemia compared with non-significant lesions (P<0.05). Table II summarizes the different quantitative and qualitative plaque characteristics and their association with FFR_{CT} ≤0.80. Univariate logistic regression analysis demonstrated that NCP [odds ratio (OR), 1.158; 95% CI, 1.103-1.215; P<0.0001], LD-NCP (OR, 1.128; 95% CI, 1.094-1.164; P<0.0001) and plaque length (OR, 1.147; 95% CI, 1.043-1.261; P=0.005) were significantly associated with lesion-specific ischemia. Finally, multivariate logistic regression revealed that LD-NCP (OR, 1.18; 95% CI, 1.105-1.256; P<0.001) was an independent predictor of lesion-specific ischemia (Table III).

Association of FFR_{CT} and lesion-specific ischemia. FFR_{CT} was found to be significantly associated with the presence of ischemia (P<0.0001) (Table II). According to the univariate regression analysis, FFR_{CT} was a significant predictor of lesion-specific ischemia (OR, 23.20; 95% CI, 11.171-48.084; P<0.0001), and was a strong independent predictor of ischemia (OR, 23.28; 95% CI, 3.505-54.561; P<0.0001) (Table III).

Combined assessment of LD-NCP and FFR_{CT} for identifying ischemia. The AUC values for the identification of FFR_{CT} ≤0.80

Table III. Univariate and multivariate logistic regression analysis of coronary CT angiography-derived plaque markers and FFR_{CT}.

	Univariate analysis		Multivariate analysis	
Variable	P-value	OR (95% CI)	P-value	OR (95% CI)
FFR_{CT} <0.80	<0.0001[a]	23.197 (11.171-48.084)	<0.0001[a]	23.276 (3.505-54.561)
Non-calcified plaque, mm^3	<0.0001[a]	1.158 (1.103-1.215)	0.0630	1.130 (0.994-1.286)
Low-density non-calcified plaque, mm^3	<0.0001[a]	1.128 (1.094-1.164)	0.0030[a]	1.178 (1.105-1.256)
Plaque length, mm	0.0050[a]	1.147 (1.043-1.261)	0.6180	0.866 (0.492-1.525)
Total plaque volume, mm^3	0.0610	1.004 (1.000-1.007)	-	-

[a]P<0.05. CT, computed tomography; FFR_{CT}, coronary CT angiography-derived fractional flow reserve; OR, odds radio; CI, confidence interval.

Table IV. Diagnostic performance of coronary CT angiography-derived plaque markers and FFR_{CT} for the identification of lesion-specific ischemia.

Variable	LD-NCP	FFR_{CT}	FFR_{CT} + LD-NCP
Area under the curve	0.789 (0.732-0.838)	0.882 (0.835-0.920)	0.918 (0.877-0.950)
Sensitivity, % (95% CI)	66.43 (58.1-74.1)	71.33 (63.2-78.6)	83.22 (76.1-88.9)
Specificity, % (95% CI)	82 (73.1-89.0)	89 (81.2-94.4)	86 (77.6-92.1)
Positive predictive value, % (95% CI)	84.1 (77.4-89.1)	90.3 (84.0-94.2)	89.5 (83.9-93.3)
Negative predictive value, % (95% CI)	63.1 (57.1-68.8)	68.5 (62.4-73.9)	78.2 (71.2-83.9)
Cut-off value	46.3 mm^3	0.80	0.41

CT, computed tomography; FFR_{CT}, coronary CT angiography-derived fractional flow reserve; LD-NCP, low-density non-calcified plaque; CI, confidence interval.

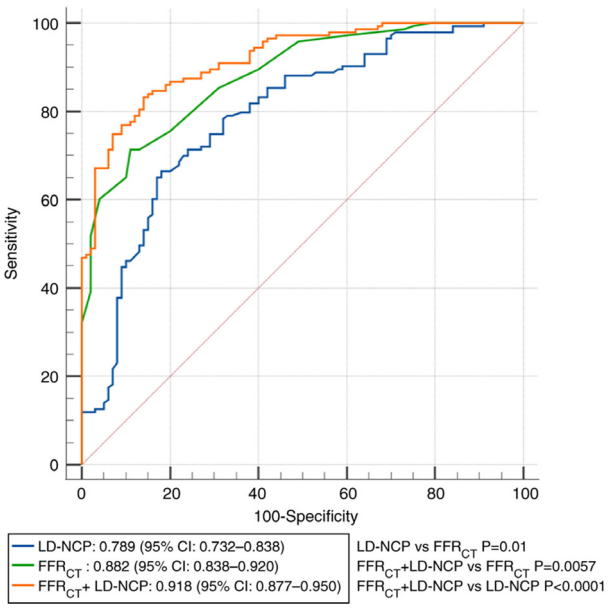

Figure 2. Diagnostic performance of FFR_{CT} and LD-NCP for the identification of lesion-specific ischemia. The receiver operating characteristic curves were created with metrics, including FFR_{CT} and LD-NCP. Model 1 included LD-NCP alone (blue line) with an AUC of 0.79; model 2 included FFR_{CT} alone (green line) with an AUC of 0.88 (P=0.01 vs. LD-NCP); and model 3 included FFR_{CT} + LD-NCP (orange line) with the highest predictive value (AUC, 0.92; P<0.0001 vs. LD-NCP; P=0.0057 vs. FFR_{CT}). FFR_{CT}, computed tomography angiography-derived fractional flow reserve; LD-NCP, low-density non calcified plaque; CI, confidence interval; AUC, area under the curve.

were 0.79 (95% CI, 0.732-0.838) for LD-NCP, 0.88 (95% CI, 0.835-0.920) for FFR_{CT} and 0.92 (95% CI, 0.877-0.950) for LD-NCP + FFR_{CT}. FFR_{CT} showed a better predictive performance relative to LD-NCP for lesion-specific ischemia (0.88 vs. 0.79; P=0.01). The addition of FFR_{CT} to LD-NCP further enhanced the predictive performance, albeit with incremental discriminatory power, compared with LD-NCP alone (0.92 vs. 0.79; P<0.0001) or FFR_{CT} alone (0.92 vs. 0.88; P=0.0057). In Fig. 2 and Table IV, analyses of the ROC curves for optimal thresholds for identifying lesion-specific ischemia are shown, as well as the results of the sensitivity, specificity, positive predictive value, negative predictive value and cut-off value calculations.

Discussion

The results of the present study have demonstrated that CCTA-based FFR_{CT} and plaque characteristics, especially LD-NCP, are predictors of lesion-specific ischemia. Importantly, FFR_{CT} and LD-NCP have been shown to be significant predictors of specific ischemia, and in combination, they synergistically increase the predictive value for ischemia compared with FFR_{CT} or LD-NCP alone.

Several studies have found a correlation between CCTA-derived plaque characteristics and ischemia, as well as significant differences between ischemia and non-significant lesions based on multiple quantitative and qualitative plaque characteristics (20-22). In the present study, it was found that plaque length, NCP volume and LD-NCP volume were not only significantly different when comparing between ischemia-causing lesions and non-significant lesions, but they were also useful in terms of predicting lesion-specific ischemia. These findings are similar to those reported by Diaz-Zamudio *et al* (23) and Iguchi *et al* (24), showing the predictive value of plaque length, NCP volume and LD-NCP volume. However, contrary to the findings of the present study, Gaur *et al* (25) reported a significant association between CCTA-derived RI and the presence of ischemia. By contrast, a different study indicated no significant correlation between plaque length or RI derived from CCTA and ischemia (26). It is likely that the determinants of study outcomes will differ significantly, which could explain the differences in results seen among studies.

LD-NCP is considered a surrogate for necrotic core plaques, and it has been shown to be useful in assessing the hemodynamic significance of coronary arteries (27). Notably, the results of the present study revealed that LD-NCP volume was an independent predictor for lesion-specific ischemia; this is a similar result to that found in a previous total-vessel study, which revealed that a higher probability of ischemia was associated with a higher LD-NCP volume (28). A retrospective study also suggested that LD-NCP volume predicts acute coronary syndromes, both on a per-patient and a per-vessel basis (29). Notably, the volume of LD-NCP was shown to be associated with the endothelial dysfunction caused by local inflammation and oxidative stress, and an increase in the LD-NCP volume led to reduced bioavailability of the vasodilator, nitric oxide, which made it difficult for the blood vessels to dilate under conditions of stress, thereby leading to ischemia (9). This mechanism may account for the ability of LD-NCP to act as a significant predictor of ischemia. However, in the presence of high-grade stenosis, plaque analysis, such as that of NCP and LD-NCP, may be less useful in terms of diagnosing ischemia (28).

Over the course of the last few decades, researchers have pursued an ideal non-invasive imaging diagnostic for ischemia. Numerous studies have shown a higher diagnostic accuracy of FFR_{CT} for lesion-specific ischemia compared with invasive FFR (30-33). In addition, FFR_{CT} based on deep-learning algorithms has been used to evaluate the hemodynamics of coronary arteries (34). A combined multicenter meta-analysis study revealed a high predictive value of FFR_{CT} for lesion-specific ischemia, with an AUC value of 0.86 (35). A similar AUC value was derived in the present study (AUC, 0.88), and deep-learning FFR_{CT} showed excellent predictive performance (OR, 23.19; P<0.0001) in terms of identifying ischemia. Additionally, FFR_{CT} provided superior discriminatory performance over LD-NCP (AUC, 0.88 vs. 0.79; P=0.006), and the addition of FFR_{CT} to LD-NCP demonstrated an incremental increase in predictive value (AUC, 0.92 vs. 0.79; P<0.0001), which is consistent with the findings of a previous study by von Knebel Doeberitz *et al* (36). However, in contrast with the present study results, a previous study found that the combination of FFR and LD-NCP was unable to increase the predictive value of FFR alone for lesion-specific ischemia (25). However, this previous study added stenosis >50% as a predictive index, and the presence of a difference in FFR_{CT} when accompanied by markedly stenotic coronary arteries may explain why the addition of FFR_{CT} had no incremental value for ischemia.

The present study had certain limitations. Firstly, the design protocol for retrospective studies and the relatively small sample size of the included study cases may have led to the existence of selection bias. Therefore, more prospective, multicenter studies are needed in the future to validate the findings. Secondly, FFR_{CT} values may vary, depending on factors such as fluid dynamics models, blood viscosity and individual differences (37), which require continuous optimization of image quality and algorithms. Combining FFR_{CT} and plaque features based on deep machine learning models may improve the identification of ischemia. Thirdly, the analysis of plaque characteristics may be limited by the resolution of CT, and the volume measurement of LD-NCP will also be affected to a certain extent (38). Therefore, in addition to improving the CT resolution, it is necessary to verify different CT scanners and different tube voltages prior to their clinical application. Fourthly, patients with severe cardiovascular disease or previous revascularization were excluded from the present study, and the predictive performance of FFR_{CT} and LD-NCP for ischemia in this group of patients requires further study. Lastly, since the automated software only calculated the total plaque length and burden, but could not measure the length of different types of plaques or the volume of blood vessels where they were located (39), the algorithm needs to be improved in the future to explore the predictive value of plaque length, volume and burden for lesion-specific ischemia.

In conclusion, CCTA-derived plaque characteristics and FFR_{CT} have been demonstrated to have predictive value in terms of identifying lesion-specific ischemia. Furthermore, the addition of FFR_{CT} to LD-NCP showed incremental discriminatory power for ischemia compared with FFR_{CT} or LD-NCP alone.

Acknowledgements

Not applicable.

Funding

The present study was supported by Zhangjiakou Key Research and Development Program Projects (grant no. 2021030D).

Availability of data and materials

The datasets used and/or analyzed during the current study are available from the corresponding author on reasonable request.

Authors' contributions

SC and LT conceived the study and wrote the manuscript. LT, FY and TD performed the experiments. LT and FL carried out the data collection and data analysis. SC and FY assessed the quality of the studies. LT, SC and FL confirm the authenticity of all the raw data. SC, LT, TD, FL and FY reviewed the results. All authors have read and approved the final manuscript.

Ethics approval and consent to participate

The Ethics Review Board of The First Affiliated Hospital, Hebei North University (Zhangjiakou, China) examined and approved the study protocol. All patients included in the study provided written informed consent.

Patient consent for publication

Not applicable.

Competing interests

The authors declare that they have no competing interests.

References

1. Basha MAA, Aly SA, Ismail AAA, Bahaaeldin HA and Shehata SM: The validity and applicability of CAD-RADS in the management of patients with coronary artery disease. Insights Imaging 10: 117, 2019.
2. Balfour PC Jr, Gonzalez JA and Kramer CM: Non-invasive assessment of low- and intermediate-risk patients with chest pain. Trends Cardiovasc Med 27: 182-189, 2017.
3. von Ballmoos MW, Haring B, Juillerat P and Alkadhi H: Meta-analysis: Diagnostic performance of low-radiation-dose coronary computed tomography angiography. Ann Intern Med 154: 413-420, 2011.
4. Li Y, Qiu H, Hou Z, Zheng J, Li J, Yin Y and Gao R: Additional value of deep learning computed tomographic angiography-based fractional flow reserve in detecting coronary stenosis and predicting outcomes. Acta Radiol 63: 133-140, 2022.
5. Wardziak Ł, Kruk M, Pleban W, Demkow M, Rużyłło W, Dzielińska Z and Kępka C: Coronary CTA enhanced with CTA based FFR analysis provides higher diagnostic value than invasive coronary angiography in patients with intermediate coronary stenosis. J Cardiovasc Comput Tomogr 13: 62-67, 2019.
6. Gohmann RF, Pawelka K, Seitz P, Majunke N, Heiser L, Renatus K, Desch S, Lauten P, Holzhey D, Noack T, *et al*: Combined cCTA and TAVR planning for ruling out significant CAD: Added value of ML-based CT-FFR. JACC Cardiovasc Imaging 15: 476-486, 2022.
7. Dwivedi G, Liu Y, Tewari S, Inacio J, Pelletier-Galarneau M and Chow BJ: Incremental prognostic value of quantified vulnerable plaque by cardiac computed tomography: A pilot study. J Thorac Imaging 31: 373-379, 2016.
8. Dey D, Schepis T, Marwan M, Slomka PJ, Berman DS and Achenbach S: Automated three-dimensional quantification of noncalcified coronary plaque from coronary CT angiography: Comparison with intravascular US. Radiology 257: 516-522, 2010.
9. Ahmadi A, Kini A and Narula J: Discordance between ischemia and stenosis, or PINSS and NIPSS: Are we ready for new vocabulary? JACC Cardiovasc Imaging 8: 111-114, 2015.
10. Ahmadi N, Ruiz-Garcia J, Hajsadeghi F, Azen S, Mack W, Hodis H and Lerman A: Impaired coronary artery distensibility is an endothelium-dependent process and is associated with vulnerable plaque composition. Clin Physiol Funct Imaging 36: 261-268, 2016.
11. Naidu SS, Rao SV, Blankenship J, Cavendish JJ, Farah T, Moussa I, Rihal CS, Srinivas VS, Yakubov SJ and Society for Cardiovascular Angiography and Interventions: Clinical expert consensus statement on best practices in the cardiac catheterization laboratory: Society for cardiovascular angiography and interventions. Catheter Cardiovasc Interv 80: 456-464, 2012.
12. de Jonge GJ, van Ooijen PM, Overbosch J, Gueorguieva AL, Janssen-van der Weide MC and Oudkerk M: Comparison of (semi-)automatic and manually adjusted measurements of left ventricular function in dual source computed tomography using three different software tools. Int J Cardiovasc Imaging 27: 787-794, 2011.
13. Chang HJ, Lin FY, Lee SE, Andreini D, Bax J, Cademartiri F, Chinnaiyan K, Chow BJW, Conte E, Cury RC, *et al*: Coronary atherosclerotic precursors of acute coronary syndromes. J Am Coll Cardiol 71: 2511-2522, 2018.
14. de Graaf MA, Broersen A, Kitslaar PH, Roos CJ, Dijkstra J, Lelieveldt BP, Jukema JW, Schalij MJ, Delgado V, Bax JJ, *et al*: Automatic quantification and characterization of coronary atherosclerosis with computed tomography coronary angiography: Cross-correlation with intravascular ultrasound virtual histology. Int J Cardiovasc Imaging 29: 1177-1190, 2013.
15. Maurovich-Horvat P, Schlett CL, Alkadhi H, Nakano M, Otsuka F, Stolzmann P, Scheffel H, Ferencik M, Kriegel MF, Seifarth H, *et al*: The napkin-ring sign indicates advanced atherosclerotic lesions in coronary CT angiography. JACC Cardiovasc Imaging 5: 1243-1252, 2012.
16. Mori H, Torii S, Kutyna M, Sakamoto A, Finn AV and Virmani R: Coronary artery calcification and its progression: What does it really mean? JACC Cardiovasc Imaging 11: 127-142, 2018.
17. Wang H, Tang ZR, Li W, Fan T, Zhao J, Kang M, Dong R and Qu Y: Prediction of the risk of C5 palsy after posterior laminectomy and fusion with cervical myelopathy using a support vector machine: an analysis of 184 consecutive patients. J Orthop Surg Res 16: 332, 2021.
18. Coenen A, Lubbers MM, Kurata A, Kono A, Dedic A, Chelu RG, Dijkshoorn ML, Gijsen FJ, Ouhlous M, van Geuns RJ and Nieman K: Fractional flow reserve computed from noninvasive CT angiography data: Diagnostic performance of an on-site clinician-operated computational fluid dynamics algorithm. Radiology 274: 674-683, 2015.
19. DeLong ER, DeLong DM and Clarke-Pearson DL: Comparing the areas under two or more correlated receiver operating characteristic curves: A nonparametric approach. Biometrics 44: 837-845, 1988.
20. Tesche C, De Cecco CN, Caruso D, Baumann S, Renker M, Mangold S, Dyer KT, Varga-Szemes A, Baquet M, Jochheim D, *et al*: Coronary CT angiography derived morphological and functional quantitative plaque markers correlated with invasive fractional flow reserve for detecting hemodynamically significant stenosis. J Cardiovasc Comput Tomogr 10: 199-206, 2016.
21. Hell MM, Dey D, Marwan M, Achenbach S, Schmid J and Schuhbaeck A: Non-invasive prediction of hemodynamically significant coronary artery stenoses by contrast density difference in coronary CT angiography. Eur J Radiol 84: 1502-1508, 2015.
22. Park HB, Heo R, Ó Hartaigh B, Cho I, Gransar H, Nakazato R, Leipsic J, Mancini GBJ, Koo BK, Otake H, *et al*: Atherosclerotic plaque characteristics by CT angiography identify coronary lesions that cause ischemia: a direct comparison to fractional flow reserve. JACC Cardiovasc Imaging 8: 1-10, 2015.

23. Diaz-Zamudio M, Dey D, Schuhbaeck A, Nakazato R, Gransar H, Slomka PJ, Narula J, Berman DS, Achenbach S, Min JK, *et al*: Automated quantitative plaque burden from coronary CT angiography noninvasively predicts hemodynamic significance by using fractional flow reserve in intermediate coronary lesions. Radiology 276: 408-415, 2015.
24. Iguchi T, Hasegawa T, Nishimura S, Nakata S, Kataoka T, Ehara S, Hanatani A, Shimada K and Yoshiyama M: Impact of lesion length on functional significance in intermediate coronary lesions. Clin Cardiol 36: 172-177, 2013.
25. Gaur S, Øvrehus KA, Dey D, Leipsic J, Bøtker HE, Jensen JM, Narula J, Ahmadi A, Achenbach S, Ko BS, *et al*: Coronary plaque quantification and fractional flow reserve by coronary computed tomography angiography identify ischaemia-causing lesions. Eur Heart J 37: 1220-1227, 2016.
26. Doris MK, Otaki Y, Arnson Y, Tamarappoo B, Goeller M, Gransar H, Wang F, Hayes S, Friedman J, Thomson L, *et al*: Non-invasive fractional flow reserve in vessels without severe obstructive stenosis is associated with coronary plaque burden. J Cardiovasc Comput Tomogr 12: 379-384, 2018.
27. Shmilovich H, Cheng VY, Tamarappoo BK, Dey D, Nakazato R, Gransar H, Thomson LE, Hayes SW, Friedman JD, Germano G, *et al*: Vulnerable plaque features on coronary CT angiography as markers of inducible regional myocardial hypoperfusion from severe coronary artery stenoses. Atherosclerosis 219: 588-595, 2011.
28. Øvrehus KA, Gaur S, Leipsic J, Jensen JM, Dey D, Bøtker HE, Ahmadi A, Achenbach S, Ko B and Nørgaard BL: CT-based total vessel plaque analyses improves prediction of hemodynamic significance lesions as assessed by fractional flow reserve in patients with stable angina pectoris. J Cardiovasc Comput Tomogr 12: 344-349, 2018.
29. Dey D, Achenbach S, Schuhbaeck A, Pflederer T, Nakazato R, Slomka PJ, Berman DS and Marwan M: Comparison of quantitative atherosclerotic plaque burden from coronary CT angiography in patients with first acute coronary syndrome and stable coronary artery disease. J Cardiovasc Comput Tomogr 8: 368-374, 2014.
30. Nakazato R, Park HB, Berman DS, Gransar H, Koo BK, Erglis A, Lin FY, Dunning AM, Budoff MJ, Malpeso J, *et al*: Noninvasive fractional flow reserve derived from computed tomography angiography for coronary lesions of intermediate stenosis severity: Results from the DeFACTO study. Circ Cardiovasc Imaging 6: 881-889, 2013.
31. Nørgaard BL, Leipsic J, Gaur S, Seneviratne S, Ko BS, Ito H, Jensen JM, Mauri L, De Bruyne B, Bezerra H, *et al*: Diagnostic performance of noninvasive fractional flow reserve derived from coronary computed tomography angiography in suspected coronary artery disease: The NXT trial (analysis of coronary blood flow using CT angiography: Next steps). J Am Coll Cardiol 63: 1145-1155, 2014.
32. Gaur S, Bezerra HG, Lassen JF, Christiansen EH, Tanaka K, Jensen JM, Oldroyd KG, Leipsic J, Achenbach S, Kaltoft AK, *et al*: Fractional flow reserve derived from coronary CT angiography: Variation of repeated analyses. J Cardiovasc Comput Tomogr 8: 307-314, 2014.
33. Li W, Wang H, Dong S, Tang ZR, Chen L, Cai X, Hu Z and Yin C: Establishment and validation of a nomogram and web calculator for the risk of new vertebral compression fractures and cement leakage after percutaneous vertebroplasty in patients with osteoporotic vertebral compression fractures. Eur Spine J 31: 1108-1121, 2022.
34. Tesche C, De Cecco CN, Baumann S, Renker M, McLaurin TW, Duguay TM, Bayer RR II, Steinberg DH, Grant KL, Canstein C, *et al*: Coronary CT angiography-derived fractional flow reserve: Machine learning algorithm versus computational fluid dynamics modeling. Radiology 288: 64-72, 2018.
35. Tang CX, Wang YN, Zhou F, Schoepf UJ, Assen MV, Stroud RE, Li JH, Zhang XL, Lu MJ, Zhou CS, *et al*: Diagnostic performance of fractional flow reserve derived from coronary CT angiography for detection of lesion-specific ischemia: A multi-center study and meta-analysis. Eur J Radiol 116: 90-97, 2019.
36. von Knebel Doeberitz PL, De Cecco CN, Schoepf UJ, Duguay TM, Albrecht MH, van Assen M, Bauer MJ, Savage RH, Pannell JT, De Santis D, *et al*: Coronary CT angiography-derived plaque quantification with artificial intelligence CT fractional flow reserve for the identification of lesion-specific ischemia. Eur Radiol 29: 2378-2387, 2019.
37. Nørgaard BL, Terkelsen CJ, Mathiassen ON, Grove EL, Bøtker HE, Parner E, Leipsic J, Steffensen FH, Riis AH, Pedersen K, *et al*: Coronary CT angiographic and flow reserve-guided management of patients with stable ischemic heart disease. J Am Coll Cardiol 72: 2123-2134, 2018.
38. Goeller M, Rahman Ihdayhid A, Cadet S, Lin A, Adams D, Thakur U, Yap G, Marwan M, Achenbach S, Dey D and Ko B: Pericoronary adipose tissue and quantitative global non-calcified plaque characteristics from CT angiography do not differ in matched South Asian, East Asian and European-origin Caucasian patients with stable chest pain. Eur J Radiol 125: 108874, 2020.
39. van Assen M, Varga-Szemes A, Schoepf UJ, Duguay TM, Hudson HT, Egorova S, Johnson K, St Pierre S, Zaki B, Oudkerk M, *et al*: Automated plaque analysis for the prognostication of major adverse cardiac events. Eur J Radiol 116: 76-83, 2019.